Available online at www.sciencedirect.com
ScienceDirect
Catalysis Today 123 (2007) 77–85
CATALYSIS TODAY
www.elsevier.com/locate/cattod

Synthesis of vinyl acetate on Pd-based catalysts

D. Kumar, M.S. Chen, D.W. Goodman *

Department of Chemistry, Texas A&M University, P.O. Box 30012, College Station, TX 77842-3012, United States

Available online 12 March 2007

Abstract

Vinyl acetate (VA) synthesis over Pd–Au catalysts is an important industrial reaction that has been studied extensively; however, there is no consensus regarding the reaction mechanism, the active site, the key intermediates, and the role of Au. Recent results from our laboratories using a combination of surface science and kinetic methods on technical and model catalytic systems have established that the VA synthesis reaction is structure sensitive, including being dependent on the Pd–Au particle size. The role of Au is to isolate surface Pd atoms into Pd monomeric sites thereby enhancing the VA formation rate and selectivity. This paper reviews the current understanding of this reaction on Pd, Pd–Au, and Pd–Sn catalysts.

Keywords: Vinyl acetate; Pd; Pd–Au; Pd–Sn

1. Introduction

Vinyl acetate (VA) is an important chemical intermediate utilized in paints, adhesives and surface coatings. The oldest VA synthesis process is the gas-phase acetoxylation of acetylene, based upon vapor phase reaction over a zinc acetate catalyst, typically supported on carbon. The reaction yields are generally very high ranging from 92 to 98% based on acetylene. However, the expense and scarcity of acetylene made this process unattractive, and in the early 1960s, several processes evolved using ethylene as a feedstock, such as the homogeneous catalytic acetoxylation of ethylene over Pd and Cu chloride catalysts [1–4]:

$$C_2H_4 + PdX_2 + HX \rightarrow [C_2H_4PdX_3]^- + H^+,$$
$$[C_2H_4PdX_3]^- + AcOH \rightarrow [C_2H_4PdX_2(OAc)]^- + HX,$$
$$[C_2H_4PdX_2(OAc)]^- \rightarrow [C_2H_4PdX(OAc)]^- + X^-,$$
$$[C_2H_4PdX(OAc)] \rightarrow CH_2CH{-}OAc + Pd + HX \quad (X = Cl)$$

Later, this process was replaced with gas phase acetoxylation of ethylene over a Pd–Au bimetallic silica-supported catalyst promoted with potassium acetate (KOAc) at a reaction temperature of 423–463 K and a total pressure of 600–1000 kPa [5–11]:

$$CH_3COOH + C_2H_4 + 0.5O_2 \rightarrow CH_3COOCHCH_2 + H_2O$$

Since, the late 1960s when the gas phase reaction of ethylene and acetic acid in the presence of oxygen to form VA over Pd-based/SiO_2 catalyst was first reported, there has been considerable interest in this reaction from the industrial sector. Recently academic researchers have shown an intense interest in investigating the mechanism of the synthesis of VA [7,12–16], although the basic aspects of the reaction were studied in the early 1970s [3,5,9]. Two commercial processes, both employing Pd-based catalysts, have been developed for the production of VA. The homogenous liquid phase process accounts for approximately 25% of the total VA production, while the heterogeneous gas phase process accounts for the remainder.

Although considerable work addressing the kinetic and mechanistic parameters has been reported on various Pd-based catalysts, there is no consensus regarding the reaction mechanism and the nature of the active sites/intermediates in VA synthesis. In this article, recent developments from our laboratories with respect to VA synthesis are summarized with an emphasis on our current understanding of the active site and the reaction mechanism.

* Corresponding author. Tel.: +1 979 845 0214; fax: +1 979 845 6822.
E-mail address: goodman@mail.chem.tamu.edu (D.W. Goodman).

0920-5861/$ – see front matter © 2007 Elsevier B.V. All rights reserved.
doi:10.1016/j.cattod.2007.01.050

2. Pd-only catalysts

In 1960, Moiseev et al. investigated the homogenous liquid-phase production of VA using a $[PdCl_2(C_2H_4)]_2$ complex catalyst [3]. The reaction was studied by vapor phase oxidation of ethylene and acetic acid by Somanos et al. in 1971 on Pd catalysts supported by SiO_2 and Al_2O_3 [9]. In this study, various parameters such as the effect of Pd dispersion, the partial pressures of the reactants/water were evaluated. Within this same time period, Nakamura and Yasui studied the mechanistic aspects of VA synthesis on Pd-based catalysts [5], investigating the promotional effect of alkali metals and the reaction orders with respect to acetic acid and ethylene. Furthermore, the heterogeneous process for VA production was shown to be preferable due to limited corrosion and the absence of chlorides.

Using Pd/SiO_2 catalysts, approximately 80–90% selectivity has been reported for VA synthesis [9,14]. In our laboratories, Pd(5.0 wt.%) and Pd(1.0 wt.%)/SiO_2 catalysts prepared by wet impregnation methods [13] were shown to have an average particle size after reduction of (4.2 ± 0.2) and (2.5 ± 0.1) nm, respectively, using transmission electron microscopy (TEM). For the same catalysts X-ray diffraction (XRD) indicated the average particle size to be 3.8 and 2.8 nm, respectively. Under reaction conditions TEM showed the average particle size to increase to 5.5 and 3.5 nm for Pd(5.0 wt.%) and Pd(1.0 wt.%), respectively. The catalysts maintained a steady activity after an initial induction period within the first 100 min. Deactivation was very slow and mainly attributed to sintering and to the formation of surface carbide [13,17]. As shown in Fig. 1, the formation of PdC_x was dependent on the particle size of the catalyst. The Pd(1.0 wt.%)/SiO_2 catalyst formed less carbide on the surface in comparison to the Pd(5.0 wt.%)/SiO_2 catalyst. The reaction rates and selectivities were higher on the 1.0 wt.% Pd with smaller particle size than on the 5.0 wt.% Pd with a larger average particle size, as reflected in Fig. 2 [18]. The dependence of the reaction rate and selectivity on the particle size indicates a degree of structure sensitivity. On the Pd(1 0 0) the rate was lower confirming that larger particles are relatively less active for VA formation [18]. The corresponding activation

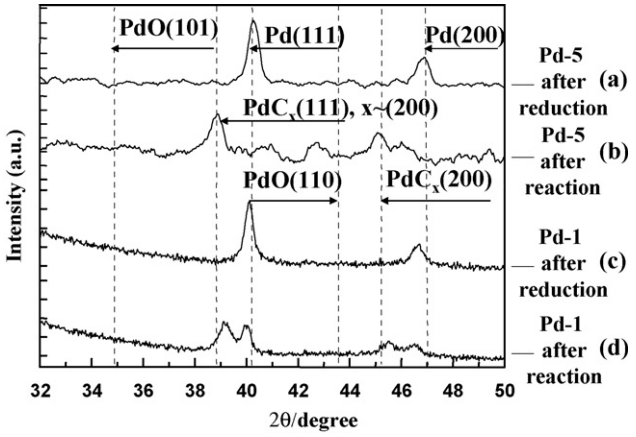

Fig. 1. XRD data for Pd-only catalysts. (a and b) Pd(5.0 wt.%)/SiO_2; (c and d) Pd(1.0 wt.%)/SiO_2; (a and c) freshly reduced; (b and d) after reaction [13].

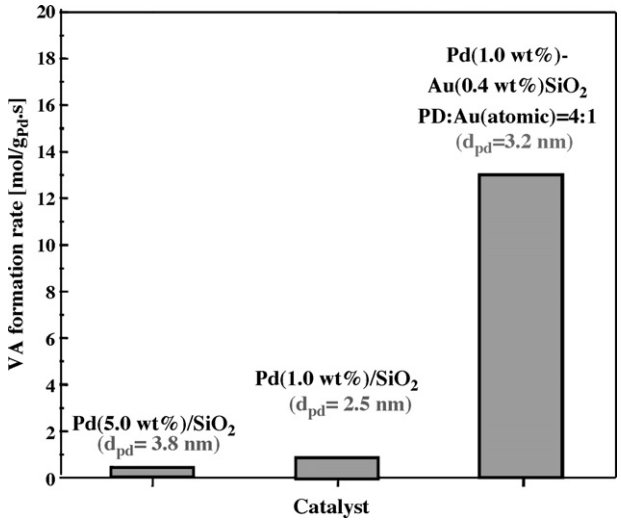

Fig. 2. VA synthesis on Pd(5.0 wt.%)/SiO_2, Pd(1.0 wt.%)/SiO_2 and Pd(1.0 wt.%)–Au(0.4 wt.%)/SiO_2 catalysts. p_{O_2} = 7.6 Torr; $p_{C_2H_4}$ = 57.0 Torr; p_{AcOH} = 12.0 - Torr; the remainder N_2; flow rate: 30–60 ml/min; temperature = 413 K; catalyst weight: 0.1–1.6 g [18].

energy (E_a) was higher (39.0 kJ/mol) for the catalyst with smaller Pd particles than for the catalyst with larger Pd particles (17.3 kJ/mol). Typically, on promoted 2.0 wt.% Pd/SiO_2 and 5.0 wt.% Pd/Al_2O_3 catalysts, the E_a was near 30.0 kJ/mol [5,9].

The reaction orders with respect to ethylene and oxygen were reported to be negative on 2.0 wt.% Pd/SiO_2 promoted with sodium acetate [9], and positive on 1.0 and 5.0 wt.% Pd/SiO_2 catalysts [13] and on 5.0 wt.% Pd/Al_2O_3 between 50 and 200 kPa [5]. A Langmuir–Hinshelwood mechanism was suggested based on the observed positive reaction order with respect to O_2 and negative order with respect to C_2H_4. The reaction orders with respect to ethylene and oxygen were independent of the particle size. The reaction order with respect to acetic acid has been a point of contention with reported values ranging from 0 to 1 [9,13,19]. On Pd(5.0 wt.%)/SiO_2 and Pd(1.0 wt.%)/SiO_2 catalysts, we found that the reaction order with respect to acetic acid is almost zero [13].

The catalytic stability was strongly dependent on the particle size with Pd(1.0 wt.%)/SiO_2 showing less deactivation compared to other catalysts after an initial induction period [18]. Overall, the kinetic parameters on Pd(1 0 0) and on supported Pd catalysts suggest a similar mechanism for VA formation [18].

3. Catalysis by Pd–Au

The reactivity of metal surfaces is a critical function of composition and structure with alloys often showing unique properties compared to the corresponding single component metals [20–22]. For example, mixtures of Pd and Au are used as catalysts for a number of applications [23–26] including hydrogen fuel cells [27] and pollution control [28]. The addition of Au to Pd significantly enhances the catalytic activity, selectivity and stability; however, the details of this promotional effect are not well understood.

Au–Pd alloys are completely miscible, with the heats of formation of Au–Pd alloys at 300 K being negative over the entire composition range; maximum stability occurs at ∼60% Au [24]. The observed large negative enthalpies are indicative of an attractive interaction between the alloy constituents and a tendency to order. The lattice parameters of Au–Pd alloys at 300 K vary from 0.389 nm for pure Pd to 0.408 nm for pure Au with a small negative deviation from Vegard's law [29]. Short-range ordering in Au–Pd alloys has been reported and reviewed by Allison et al. [24]. Early work on the properties of these Pd–Au catalysts concluded that the 0.6 d-band vacancies of pure Pd fill at an alloy composition of ∼60% Au, a results that stimulated studies of the catalytic properties of Au–Pd mixtures at this critical composition, e.g., ortho, *para*-hydrogen conversion [30]. However, in surveying a number of reactions, the consensus is that surface composition is more important for adsorption and catalysis than is the bulk electronic structure [12,24,31–34]. There is still considerable uncertainty in the interpretation of the surface properties, since the surface composition can differ markedly from the bulk, and the surface atoms can be quite mobile under reaction conditions. In any case, theoretical calculations have shown a correlation among surface strain, adsorption energy, and activation barriers for reaction [35].

3.1. Supported catalysts

Debate regarding the catalytic active site for VA synthesis has focused on whether Pd is present as Pd^0 or Pd^{2+}. Moiseev et al. have argued that the active site consists of Pd^0, which catalyze very selectively the vinyl acetate reaction [3]. More convincingly, the active site was proposed to contain an acetate species [36,10,5], $Pd(OAc)_2$, formed from acetic acid adsorption [19]. The proposed reaction mechanism is [10]:

$$C_2H_4 + 2Pd \Leftrightarrow CH_2{-}CH{-}Pd + PdH,$$

$$O_2 + 2Pd \Leftrightarrow 2Pd{-}O,$$

$$CH_3COOH + Pd \Leftrightarrow Pd{-}CH_3COOH,$$

$$Pd{-}CH_3COOH + Pd{-}O \Leftrightarrow Pd{-}O{-}COCH_3 + Pd{-}OH,$$

$$Pd{-}O{-}COCH_3 + CH_2CH{-}Pd \Leftrightarrow Pd{-}CH_2CHOCOCH_3 + Pd,$$

$$Pd{-}CH_2CHOCOCH_3 \Leftrightarrow Pd + CH_2CHOCOCH_3,$$

$$Pd{-}OH + PdH \Leftrightarrow Pd{-}OH_2 \Leftrightarrow Pd + H_2O$$

It is probable that a gas–solid mechanism is involved in this reaction. However, there is strong evidence showing that a liquid phase-like mechanism is also occurring under reaction conditions. Under typical industrial operating conditions, the absorption of acetic acid and water on the support can be substantial [9]. An absorbed acetic acid liquid layer, with approximately three monolayers in thickness at temperatures comparable to industrial conditions on Pd/Cd/silica and Pd/Au/silica catalysts, was evident in isotopic transient kinetics and TPD studies [37]. The presence of Pd and alkali metal acetate (KOAc in particular) enhances the adsorption of acetic acid. KOAc, known to form a dimer species with acetic acid, is essential for a liquid phase [38] in immobilizing the acetic acid, which, in turn, increases the reaction rate for vinyl acetate and suppresses direct ethylene combustion [6,9].

Based on Monte Carlo simulations, Neurock et al. [39,15] have proposed that the critical ensemble required to couple ethylene and acetate to VA consists of several Pd atoms. The addition of Au improves the activity for vinyl acetate synthesis by approximately a factor of 2 and the selectivity by approximately 5%. Comparative kinetic studies of VA synthesis were carried out for Pd(1.0 wt.%)/SiO_2 and Pd(1.0 wt.%)–Au(0.5 wt.%)/SiO_2 catalysts, with the highly dispersed metal particles (Pd and Pd–Au) characterized by XRD and TEM-EDS [14]. For Pd–Au catalysts, the reaction orders with respect to C_2H_4 and oxygen are both positive. High surface area SiO_2 supported Pd and Pd–Au VA synthesis catalysts show that addition of approximately 20 at.% of Au enhances the VA formation rate by a factor of 16 as shown in Fig. 2. This change in the kinetic parameters is attributed to a change in the electronic and geometric properties of Pd upon alloying with Au. Confirming the observations of Macleod et al. [7] a reduction in the Pd concentration leads to an increase in the Au surface concentration. The formation of Pd carbide (PdC_x) during the synthesis of VA was also investigated over a Pd–Au/SiO_2 mixed-metal catalyst [17]. XRD and XPS data showed no PdC_x species at the surface of the Pd–Au catalyst, i.e., alloying of Au with Pd is very effective in preventing PdC_x formation in Pd-based catalysts for VA synthesis.

An early study directly addressing the role of Au in enhancing the VA reaction rate is that by Provine et al. [6]. While noting that there is indeed an increase in the production of VA, it was reported that the stability of certain surface species was altered with the addition of Au and that Au suppresses the formation of CO via combustion of acetic acid. The addition of Au also enhanced the production of VA by facilitating product desorption. While corroborating this, Lambert and coworkers further proposed that Au inhibits the decomposition of VA [7]. The addition of Au also was purported to enhance the formation of a monodentate surface acetate species at 1735 cm^{-1}. This species, proposed as a key reaction intermediate, was observed under reaction conditions on a working Pd catalyst by Augustine and Blitz [19].

The commercial VA synthesis catalyst, Pd–Au–K/SiO_2, contains approximately 1 wt.% of Au and Pd with a 4:1 Pd:Au atomic ratio, and 2.5 wt.% of potassium acetate [7,14]. For a commercial Pd–Au–K/SiO_2 catalyst, progressive loss of activity occurs during operation, restricting the lifetime. Detailed XRD and HREM/EDX investigations [7] show that fresh catalysts contain Pd in two forms: Pd–Au alloy particles 4–5 nm in diameter with a Pd:Au ratio of 2:3 and a very highly dispersed Pd metal component corresponding to ∼85% of the total Pd loading. As a consequence, the alloy particles are far more Au-rich (60 at.% Au) than expected from the metal loadings (∼20% Au). After aging (deactivation), pronounced sintering of the Pd–Au alloy particles and the appearance of Pd acetate were observed, but without significant change in composition of the alloy particles. It was found that high reaction temperatures as well as high oxygen partial pressures favor deactivation while both the ethylene concentration and initial GHSV influence very little the deactivation rate [40].

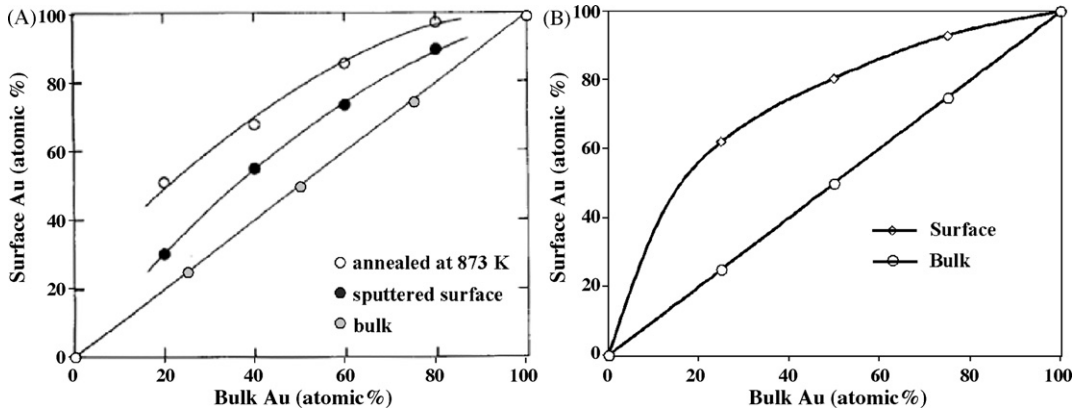

Fig. 3. Surface vs. bulk compositions for Au–Pd polycrystalline alloys (A) (●) steady-state sputtered surfaces, (○) annealed at 973 K [43], and (B) for Au–Pd thin films on Mo(1 1 0) [45].

3.2. Surface versus bulk composition

A number of studies have shown that the surface composition of Au–Pd mixtures differs from the respective bulk composition, with the surface being enriched in Au [41–44]. Surface enrichment in Au is consistent with Au having a much lower surface free energy compared with Pd. AES studies of Au–Pd alloy surfaces containing various bulk compositions show that Au is significantly enriched in an annealed surface [42]. These results have been confirmed using low-energy ion scattering spectroscopy (LEIS), a technique particularly sensitive to the top-most surface layer, as shown in Fig. 3(A) [43]. The effect of annealing temperatures on the surface composition of Pd and Au (5 ML Pd/5 ML Au/Mo(1 1 0) and 5 ML Au/5 ML Pd/Mo(1 1 0)) was investigated using LEIS as shown in Fig. 4 [45]. After annealing to higher temperature inter-diffusion of Pd–Au is evident. For example, at 800 K the surface is significantly enhanced in Au relative to the bulk. Between 700 and 1000 K, a stable surface alloy composition of $Pd_{0.2}Au_{0.8}$ is formed for a 50–50 bulk mixture of Pd and Au, independent of the deposition sequence of the Pd and Au. LEIS data were obtained at various Pd and Au bulk ratios to produce a Pd–Au surface phase diagram. As shown in Fig. 3(B) the LEIS data for Au–Pd thin films supported on a refractory single crystal Mo(1 1 0) surface are in excellent agreement with the corresponding data measured for bulk alloys (Fig. 3(A)) [42–44].

There are only a few examples where Au–Pd alloy single crystal surfaces have been examined using a surface-layer sensitive technique [46,47]. LEIS studies of Au_3Pd(1 1 3) [47] and Au_3Pd(1 0 0) [46] surfaces show these surfaces to consist essentially of a Au layer; Pd is found only within the second atomic layer. Preferential surface segregation of one component is common in metal alloy surfaces [48,49] and, in particular, all Au-containing alloys show preferential surface segregation of Au [49–51].

Based on the surface stabilities of Au–Pd alloys, epitaxial growth of a Pd monolayer on Au(1 1 1) should be thermodynamically unstable even at rather moderate temperatures. Koel and coworkers [52] carried out detailed investigations of Pd overlayers on Au(1 1 1) using AES and LEIS. Following the deposition of Pd at 150 and 300 K, results consistent with a van der Merwe growth mode, i.e., layer-by-layer. At 500 K, however, the Pd AES intensity is markedly smaller while the Au AES value is larger than the corresponding values at 150 and 300 K. These observations qualitatively indicate alloying or inter-diffusion of a Pd monolayer at 500 K. Lambert and coworkers [53] have addressed Pd submonolayers on Au(1 1 1)-$(22 \times \sqrt{3})$, where Pd islands initially nucleate and grow at the elbows near the surface edge dislocations of the Au herringbone reconstruction. A morphological evolution of these islands with increasing Pd coverage was observed and provides an excellent explanation for their catalytic behavior.

Maroun et al. [54] using high resolution STM images obtained from Pd–Au alloy surfaces prepared by electrochemically co-deposition of Pd and Au onto Au(1 1 1), clearly resolved two types of atoms with different apparent heights and

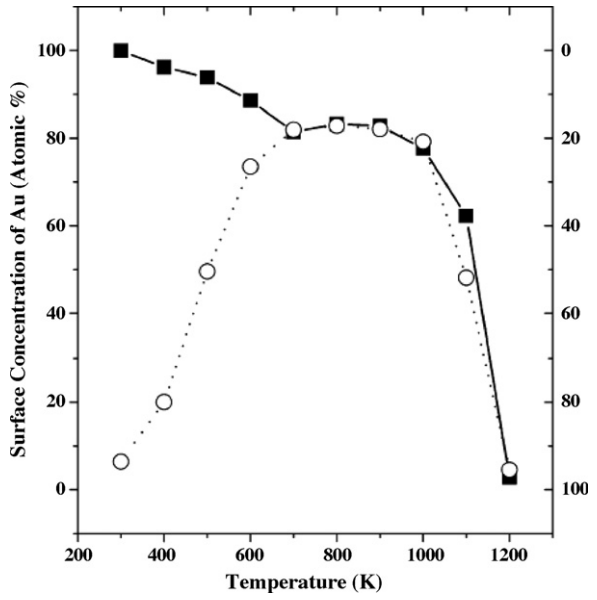

Fig. 4. Surface concentrations of Pd and Au of 5 ML Pd/5 ML Au/Mo(1 1 0) (○) and 5 ML Au/5 ML Pd/Mo(1 1 0) (■) as a function of annealing temperatures [45].

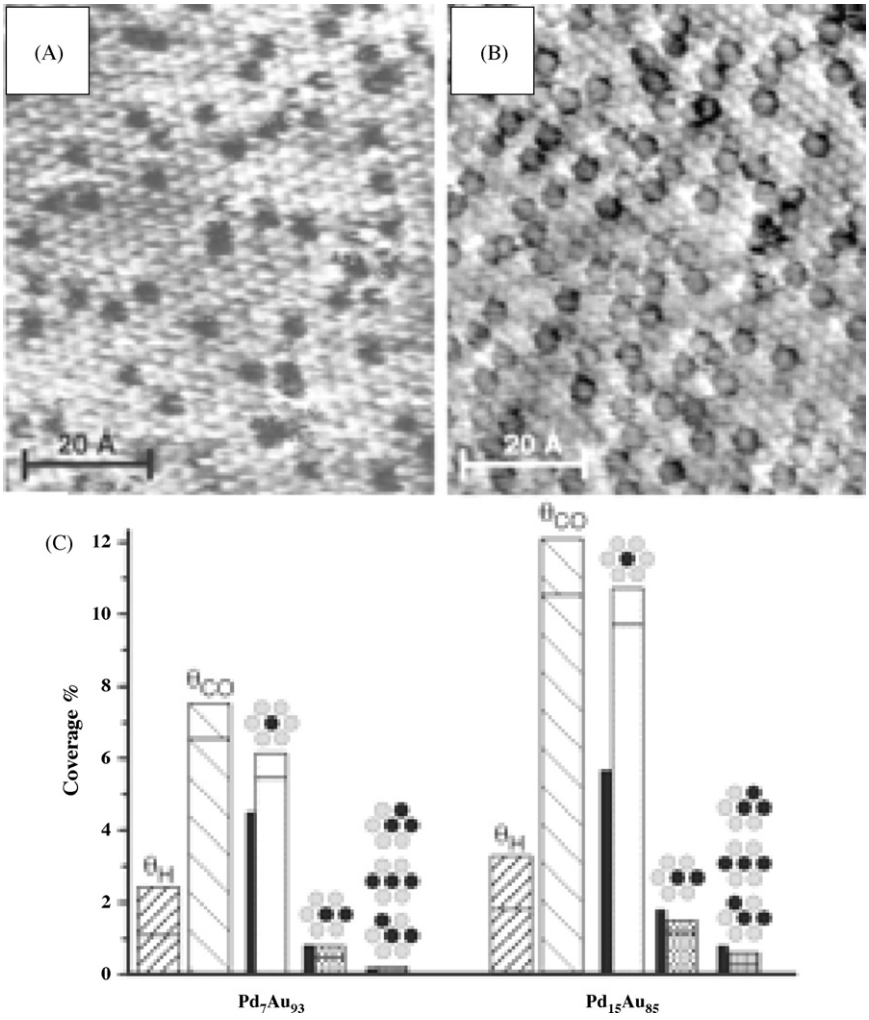

Fig. 5. In situ atomic resolution STM images of PdAu alloys electrodeposited on Au(1 1 1) for (A) $Pd_{07}Au_{93}$ and (B) $Pd_{15}Au_{85}$. Pd atoms appear larger and, depending on tunneling conditions, brighter or darker than Au atoms. (C) Surface coverages of Pd monomers, dimers, and trimers, as obtained from atomically resolved STM images [54].

shapes, arranged in a hexagonal lattice with a lattice spacing equal to that of Au(1 1 1) (see Fig. 5). Varga and Hetzendorf [44] also resolved two types of atoms with apparent chemical contrast on Au_3Pd(1 0 0) surface (see Fig. 6). The formation of surface isolated Pd sites together with some dimers and trimers were evident. These STM images with atomic contrast clearly show that a single, uniform Au–Pd alloy phase with a disordered metal-atom arrangement can be formed without phase separation into Pd and Au domains.

Recent studies in our laboratories using infrared reflection absorption spectroscopy (IRAS) with CO as a probe molecule have clearly demonstrated the formation of isolated Pd surface sites surrounded by Au on Au–Pd thin films supported on a Mo(1 1 0) surface [45] and for Pd on Au(1 1 1) [12]. As shown in Fig. 7, at room temperature after deposition of Pd on Au(1 0 0) and Au(1 1 1), CO vibrational features corresponding to adsorption on the twofold bridge and threefold hollow sites are evidenced [45]. These results are consistent with previous reports confirming the formation of Pd overlayers on Au(1 1 1) and Au(1 0 0). After annealing these samples to 600 K or higher, the CO features corresponding to bridging and threefold hollow sites disappear. This is also accompanied by an increase in the intensity of the feature corresponding to CO adsorption on atop sites of Pd. These results demonstrate that much of the deposited Pd atoms diffuse into the bulk of the catalysts forming a Pd–Au alloy with a limited number of Pd atoms isolated as Pd monomers, i.e., Au_4Pd on Au(1 0 0) and Au_6Pd on Au(1 1 1), after annealing. Thus, the formation of isolated Pd atoms surrounded by Au atoms was observed. Furthermore, the concentration of isolated Pd monomers depends on the Pd–Au bulk concentration and the annealing temperature. However, it should be noted that in the reaction conditions Pd may be pulled to the surface due to the adsorption of acetic acid [55].

3.3. Model catalysts

From recent single crystal studies in our laboratory, details regarding the Pd–Au ensemble required for VA synthesis have been revealed [12]. In these studies Pd was vapor deposited onto two gold substrates, Au(1 0 0) and Au(1 1 1), followed by annealing for 10 min at 550 K. Infrared reflection absorption

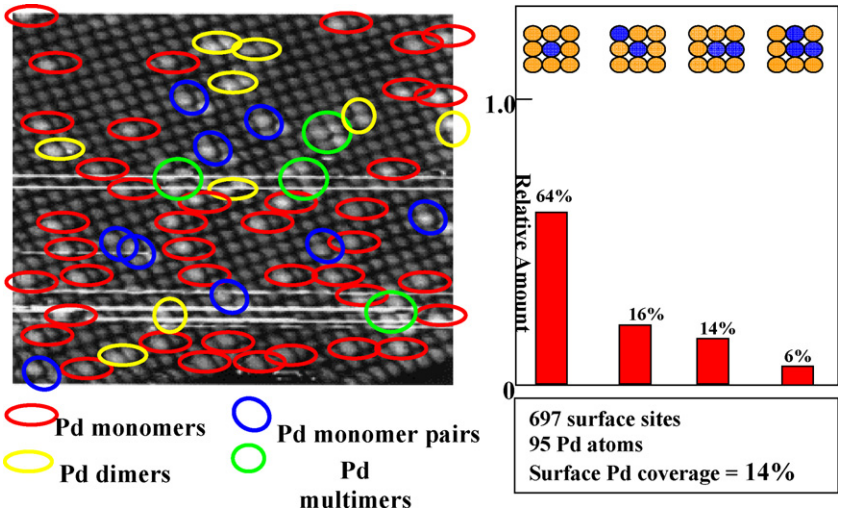

Fig. 6. Atomic resolution STM images of $Au_3Pd(1\ 0\ 0)$ surface (left). Pd atoms appear larger and brighter as indicated by circles or ellipses. The surface Pd coverage is 14%, in which the relative amounts of monomer, monomer pair, dimer and those ensembles of more than two contiguous Pd atoms are shown in the histogram (right) [44].

spectroscopy (IRAS) and CO adsorption on Pd/Au(1 0 0) and Pd/Au(1 1 1) surfaces confirmed that Pd atoms form monomers within a Au-rich surface. These Pd/Au(1 0 0) and Pd/Au(1 1 1) catalysts were used to investigate the rate of formation of VA. The reaction rate increased to a maximum at a coverage of 0.1 ML of Pd on Au(1 0 0) and decreased with a further increase in the Pd coverage (see Fig. 8) up to 1.0 ML at which coverage the reaction rate is essentially the same as that for Pd(1 0 0). For the optimum surface of 0.1 ML of Pd, the density of Pd monomers is the highest, consistent with Pd monomers being the active sites for the formation of VA on Pd/Au surfaces.

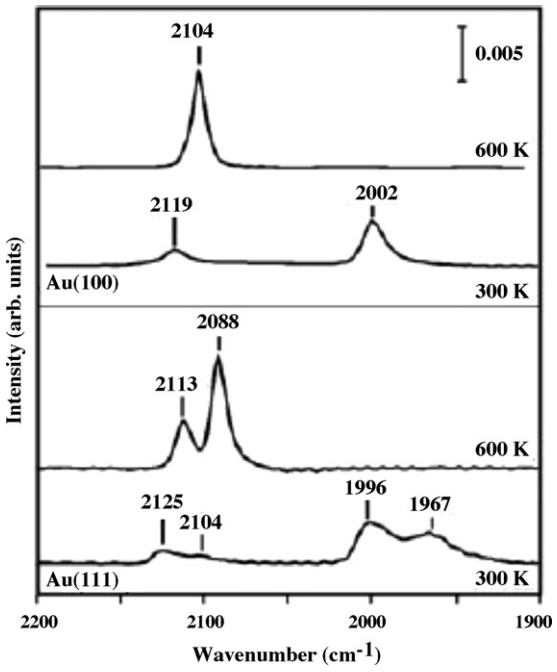

Fig. 7. IRAS spectra after CO adsorption at 90 K on 4 ML Pd/Au(1 0 0) and 4 ML Pd/Au(1 1 1). Pd was deposited on Au(1 0 0) and Au(1 1 1) at 90 K and subsequently annealed to 300 and 600 K for 10 min each [12].

The VA synthesis rate on a Au-only surface is insignificant compared to the Pd-only surface, therefore it is then straightforward to measure the VA reaction rate for the Pd–Au alloy catalysts with respect to the atomic fraction of Pd on the surface, as shown in Fig. 9. The formation rate per Pd on Au(1 0 0) surface varies with the amount of Pd on the surface with the maximum in the activity occurring at a coverage of 0.07 ML. While a decrease is apparent in the reaction rate with an increase or decrease in the coverage of Pd on Au(1 0 0), a quite different behavior is found following deposition of Pd onto a Au(1 1 1) surface. A continuous increase in the reaction rate is observed with a decrease in the surface coverage of Pd on Au(1 1 1). These data for VA formation rate on Pd on Au(1 0 0)

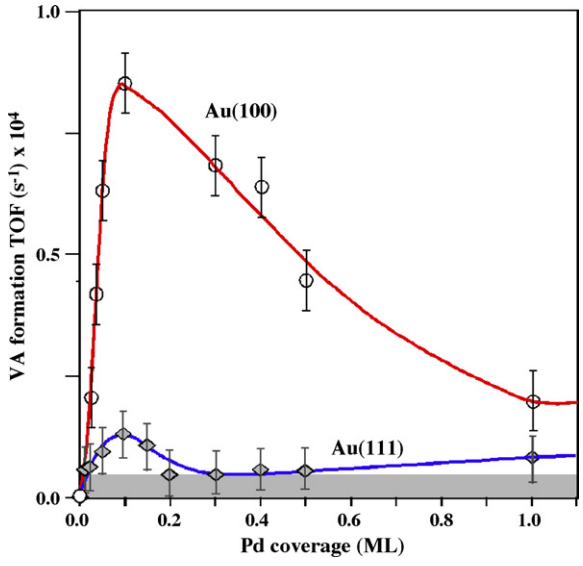

Fig. 8. VA formation rate as a function of the Pd coverage on Au(1 0 0) and Au(1 1 1) surfaces. TOFs are calculated with respect to (1 × 1) surface unit. Pd was deposited on the respective surface at 300 K and annealed to 600 K for 10 min. C_2H_4 = 8 Torr, O_2 = 2 Torr, CH_3COOH = 4 Torr, reaction temperature = 453 K, reaction time = 3 h [12].

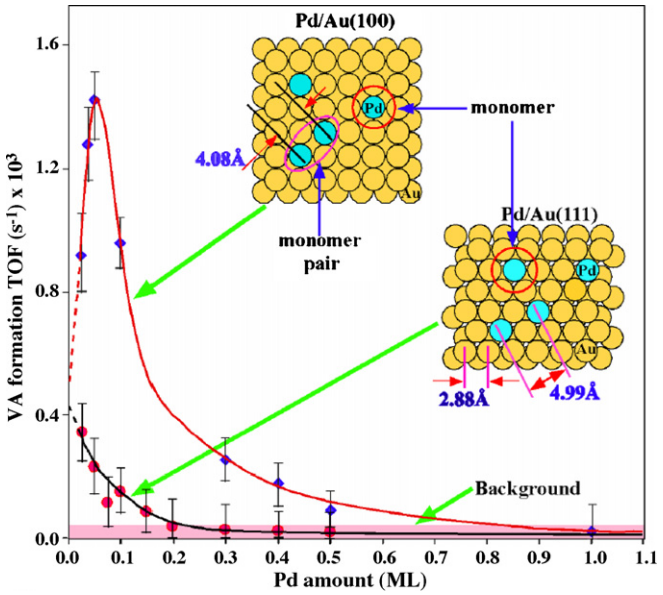

Fig. 9. Vinyl acetate (VA) formation rates as a function of Pd coverage. The TOFs are computed with respect to the Pd atom concentration. Pd was deposited on the respective surface at 300 K and annealed to 600 K for 10 min. C_2H_4 = 8 Torr, O_2 = 2 Torr, CH_3COOH = 4 Torr, reaction temperature = 453 K, reaction time = 3 h. The error bars are based on background rate data. The inserts show Pd monomers and monomer pairs on the Au(1 0 0) and Au(1 1 1) [12].

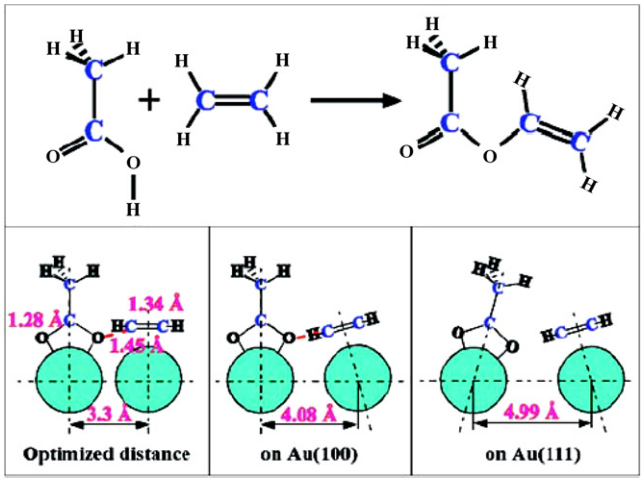

Fig. 10. Schematic for VA synthesis from acetic acid and ethylene. The optimized distance between the two active centers for the coupling of surface ethylene and acetate species to form VA is 3.3 Å. With lateral displacement, coupling of an ethylene and acetate species on a Pd monomer pair is possible on the Au(1 0 0), but unlikely on the Au(1 1 1) [12].

and Au(1 1 1) surfaces are strong evidence for isolated Pd atoms being the active sites for the reaction. The apparent difference in the per Pd reaction rates for Au(1 0 0) and Au(1 1 1) surfaces also indicates that a pair of non-contiguous Pd monomer sites, rather than a single isolated site, is required for VA formation.

Two different reaction mechanisms have been proposed for VA synthesis. The adsorption and subsequent activation of ethylene to form vinyl species which then couples with the coadsorbed acetate species to form VA is one proposed mechanism [5]. In a second mechanism, adsorbed ethylene reacts with an adsorbed acetate nucleophile to form as intermediate species, ethyl-acetate. This species then undergoes β-CH elimination to form VA [9,15]. Both mechanisms invoke coupling of acetate and ethylene species as the rate-limiting step [5,9,15]. Hence a correlated pair of Pd sites is required for the formation of VA. Considering the bond lengths of adsorbed ethylene and acetate species, the optimized distance between two active sites is 3.3 Å. Au(1 0 0) defines the distance between a pair of Pd monomers to be 4.08 Å while Au(1 1 1) defines this distance to be 4.99 Å, a prohibitively long distance for coupling of these two reactive intermediates. The reaction rate therefore on Pd/Au(1 1 1) is much lower than that on Pd/Au(1 0 0) as evidenced in Fig. 9. The bonding and relative distances involved between reacting species is shown schematically in Fig. 10.

The pair of isolated Pd sites, while aiding in the formation of VA by providing the optimum required spacing for coupling of the surface acetate and ethylene species, was also proposed to suppress the formation of reaction by-products, such as CO and CO_2, thus improving the overall selectivity. CO is a by-product or reaction intermediate in VA synthesis [15]. Since, CO binds more tightly to sites containing contiguous Pd atoms compared to an isolated Pd site (Fig. 11(A)) [45], CO is likely a more effective poison for larger Pd ensembles. Hence, addition of Au to Pd was found to significantly suppress carbon deposition via reactant and product decomposition which, in turn, leads to a reduction in dehydrogenation rates that favors selective acetoxylation [17,56–59].

In addition to CO, CO_2 is also produced as a by-product in VA synthesis due to the combustion of various reactants and the VA product [37,59]. In general, there has been a long-standing debate as to the contributions of the individual reactants, i.e., ethylene and acetic acid, toward the formation of CO_2. While some researchers have concluded that CO_2 is mainly produced from ethylene [5,9], others have argued that acetic acid also contributes to the formation of CO_2 [37]. On Pd–Cd/SiO_2 and Pd–Au/SiO_2 promoted with K^+, Crathorne et al. [37] have reported that acetic acid and ethylene contribute equally to the formation of CO_2. Using various types of catalysts, such as unsupported Pd, Pd supported on Al_2O_3, with the latter promoted with K, Nakamura and Yasui asserted that CO_2 is primarily produced from ethylene [5]. Also, Somanos et al. reached a similar conclusion using Pd supported on Al_2O_3 and SiO_2 catalysts in the presence and absence of acetic acid [9]. Ethylene oxidation was investigated in the presence and absence of acetic acid and VA on Pd(5.0 wt.%)/SiO_2 catalyst at conditions close to those used for VA synthesis [59]. In the presence and absence of acetic acid (2.0 kPa) there was no obvious change in the reaction kinetic parameters. It was concluded that within the temperature range of 413–453 K and at pressures ranging between 1.0 and 10.0 kPa of O_2 and 5.0–15.0 kPa of C_2H_4, CO_2 is primarily derived from ethylene combustion.

The formation of isolated Pd monomer sites influences the adsorption properties of ethylene as well. Indeed, TPD has shown that ethylene and acetic acid bond significantly less

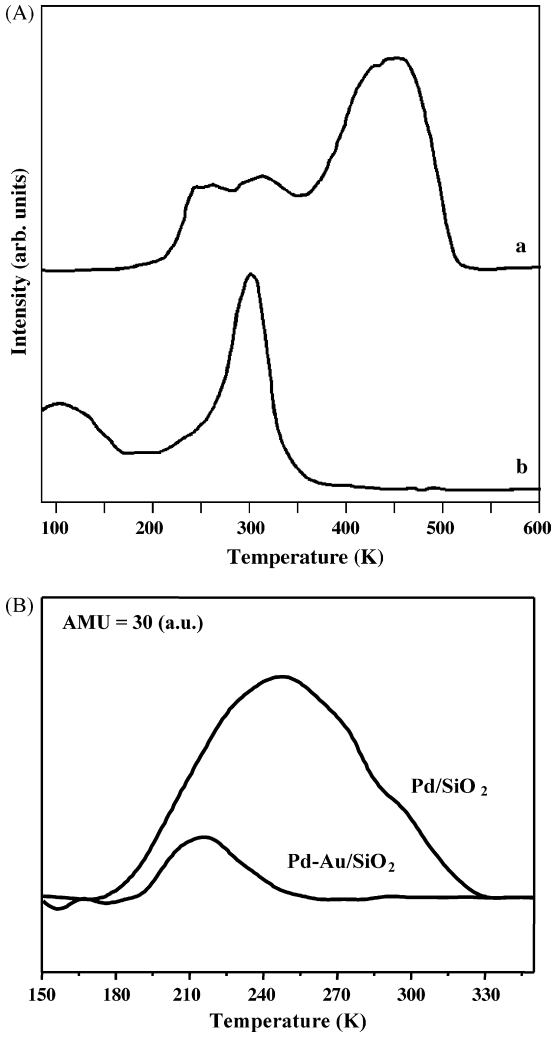

Fig. 11. (A) TPD of CO on: (a) 10 ML Pd/Mo(1 1 0) and (b) 5 ML Pd/5 ML Au/Mo(1 1 0) annealed to 800 K for 20 min [45,59]. (B) TPD of C_2D_4 from supported Pd and Pd–Au bimetallic clusters [59].

strongly to a Pd monomer compared to a site containing contiguous Pd atoms [60] (Fig. 11(B)). On continuous Pd sites a di-σ bonded ethylene species and an ethylidyne species were observed [61]. The decomposition of these species leads to the formation of carbon, whereas the addition of Au inhibits the dissociation of ethylene, consequently forming less carbon and extending the activity of the catalyst.

4. VA synthesis using Pd–Sn surfaces

The epitaxial growth of metals on refractive metal surfaces has been used to study the properties of thin metal films. For example, Pd and Sn grow layer-by-layer on several metal substrates [62,63]. Recently Sn was vapor deposited onto a 4.0 ML thick film of Pd and annealed to 600 K for 1.0 min [64]. For VA reaction times of 3.0 h, a maximum rate expressed per Pd was found after deposition of approximately 0.5 ML of Sn, which is significantly higher relative to a Pd-only surface. Further increase in the Sn coverage leads to a reduction in the VA formation rate, as shown in Fig. 12. A Sn coverage of

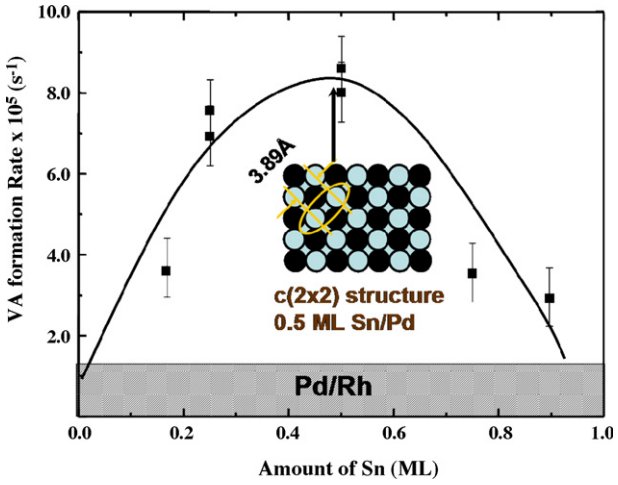

Fig. 12. VA formation rate normalized to per Pd site basis on Sn/4.0 ML Pd/Rh(1 0 0) annealed to 600 K for 60 s. Reaction at 450 K; $p_{O_2} = 2.0$ Torr; $p_{C_2H_4} = 9.0$ Torr; $p_{AcOH} = 4.0$ Torr; time = 3 h [63].

0.5 ML corresponds to a $c(2 \times 2)$ Pd–Sn structure whose formation has been observed for Sn on Pd(1 0 0) using low energy electron diffraction (LEED) [65]. Similar results have been reported by the Koel and Lambert groups on Pd(1 1 1), Pd(1 1 0), Pt(1 1 1) and Pt(1 0 0) surfaces [61,62,66–68]. The total density of Pd monomer pairs is maximized at this coverage and the distance between each isolated Pd monomer is 3.89 Å. In fact, subsequent to the formation of the $c(2 \times 2)$ structure, the distance between any two contiguous Pd atoms is identical. Since it has been proposed that a pair of Pd monomers suitably spaced act as the active sites [12], the VA formation rate should be maximized for a $c(2 \times 2)$ Sn–Pd structure, as is observed.

With further increase in Sn coverage the VA formation rate decreases slightly likely due to the decrease in the Pd monomer density and the formation of Sn islands on the surface of the catalyst. Excess Sn diffusing into the subsurface region of Pd and a Sn overlayer could influence the adsorption and reaction of neighboring Pd atoms and lead to a decrease in the overall activity.

5. Conclusions

A combination of surface science and kinetic methods have been used to study the role of Au in Pd–Au alloy catalysts for VA synthesis. The reaction has been shown to be structure sensitive including a strong dependence on metal particle size. Furthermore, addition of Au to a Pd catalyst significantly enhances the VA formation rate while reducing the amount of carbon formed on the surface. LEIS was used to investigate the surface versus bulk composition for Pd–Au surfaces. Using IRAS and CO as a probe, Au has been shown to isolate surface Pd into monomeric sites which have been proposed to be the active site for the formation of VA. A pair of such isolated Pd monomers is required for the adsorption of acetic acid and ethylene, with the distance between the constituent monomers being critical. Hence, while separating Pd atoms on the surface into monomer sites, Au also reduces the formation of undesirable surface

species and products. Utilization of Pd–Sn surfaces for the formation of VA is further confirmation that isolated Pd monomeric sites are indeed the active site for this reaction.

Acknowledgements

We greatly acknowledge the support of this work by the Department of Energy, Office of Basic Energy Sciences, Division of Chemical Sciences, and the Robert A. Welch Foundation.

References

[1] G.S. Grover, R.V. Chaudhari, Chem. Eng. J. 32 (1986) 93.
[2] D.D. Kragten, R.A. van Santen, M.K. Crawford, W.D. Provine, J.J. Lerou, Inorg. Chem. 38 (1999) 331.
[3] I.I. Moiseev, M.N. Vargaftic, Y.K. Syrkin, Dokl. Akad. Nauk Az. SSR 133 (1960) 377.
[4] C.R. Reilly, J.J. Lerou, Catal. Today 41 (1998) 433.
[5] S. Nakamura, T. Yasui, J. Catal. 17 (1970) 366.
[6] W.D. Provine, P. Mills, J.J. Lerou, Stud. Surf. Sci. Catal. 101 (1996) 191.
[7] N. Macleod, J.M. Keel, R.M. Lambert, Appl. Catal. A 261 (2004) 37.
[8] W. Schwerdt, Chem. Ind. 45 (1968) 1559.
[9] B. Samanos, P. Boutry, R. Montarna, J. Catal. 23 (1971) 19.
[10] S. Nakamura, T. Yasui, J. Catal. 23 (1971) 315.
[11] M.L. Luyben, B.D. Tyreus, Comput. Chem. Eng. 22 (1998) 867.
[12] M.S. Chen, D. Kumar, C.W. Yi, D.W. Goodman, Science 310 (2005) 291.
[13] Y.F. Han, D. Kumar, D.W. Goodman, J. Catal. 230 (2005) 353.
[14] Y.F. Han, J.H. Wang, D. Kumar, Z. Yan, D.W. Goodman, J. Catal. 232 (2005) 467.
[15] M. Neurock, J. Catal. 216 (2003) 73.
[16] D. Stacchiola, F. Calaza, F. Burkholder, W.T. Tysoe, J. Am. Chem. Soc. 126 (2004) 15384.
[17] Y.F. Han, D. Kumar, C. Sivadinarayana, A. Clearfield, D.W. Goodman, Catal. Lett. 94 (2004) 131.
[18] D. Kumar, Y.-F. Han, M.S. Chen, D.W. Goodman, Catal. Lett. 106 (2006) 1.
[19] S.M. Augustine, J.P. Blitz, J. Catal. 142 (1993) 312.
[20] J.H. Sinfelt, Bimetallic Catalysts: Discoveries, Concepts and Applications, Wiley, New York, 1983.
[21] R.L. Moss, L. Whally, Advances in Catalysis, Academic Press, New York, 1972.
[22] V. Ponec, Adv. Catal. 32 (1983) 149.
[23] R. Abel, P. Collins, K. Eichler, I. Nicolau, D. Peters, in: G. Ertl, H. Knozinger, J. Weitkamp (Eds.), Handbook of Heterogeneous Catalysis, vol. 5, Wiley/VCH, Weinheim, 1997, p. 2298.
[24] E.G. Allison, G.C. Bond, Catal. Rev. 7 (1972) 233.
[25] P.N. Rylander, Catalytic Hydrogenation in Organic Synthesis, Academic Press, London, 1979.
[26] A.M. Venezia, V. La Parola, B. Pawelec, J.L.G. Fierro, Appl. Catal. A 264 (2004) 43.
[27] D.L. Trimm, Z.I. Onsan, Catal. Rev. 43 (2001) 31.
[28] M. Bonarowska, A. Malinowski, W. Juszczyk, Z. Karpinski, Appl. Catal. B 30 (2001) 187.
[29] A. Maeland, T.B. Flanagan, Can. J. Phys. 42 (1964) 2364.
[30] A. Couper, D.D. Eley, Discuss. Faraday Soc. 8 (1950) 172.
[31] C.J. Baddeley, R.M. Ormerod, A.W. Stephenson, R.M. Lambert, J. Phys. Chem. 99 (1995) 5146.
[32] D.D. Eley, P. Luetic, Trans., Faraday Soc. 53 (1957) 1483.
[33] G. Reinacker, S. Engels, Z. Anorg. Allg. Chem. 336 (1965) 259.
[34] W.M.H. Sachtler, P. van Der Planck, Surf. Sci. 18 (1969) 62.
[35] M. Mavrikakis, B. Hammer, J.K. Norskov, Phys. Rev. Lett. 81 (1998) 2819.
[36] H. Debellefontaine, J. Besombes-Vailhe, J. Chim. Phys. 75 (1978) 801.
[37] E.A. Crathorne, D. MacGowan, S.R. Morris, A.P. Rawlinson, J. Catal. 149 (1994) 254.
[38] Handbook of Chemistry and Physics, 48th ed., Chemical Rubber, 1967.
[39] M. Neurock, W.D. Provine, D.A. Dixon, G.W. Coulston, J.J. Lerou, R.A. Vansanten, Chem. Eng. Sci. 51 (1996) 1691.
[40] Q. Smejkal, D. Linke, U. Bentrup, M.-M. Pohl, H. Berndt, M. Baerns, A. Bruckner, Appl. Catal. A 268 (2004) 67.
[41] S.M. Foiles, J. Vac. Sci. Technol. A 5 (1987) 889.
[42] A. Jablonski, S.H. Overbury, G.A. Somarjai, Surf. Sci. 65 (1977) 578.
[43] D.G. Swartzfager, S.B. Ziemecki, M.J. Kelly, J. Vac. Sci. Technol. 19 (1981) 185.
[44] P. Varga, G. Hetzendorf, Surf. Sci. 162 (1985) 544.
[45] C.W. Yi, K. Luo, T. Wei, D.W. Goodman, J. Phys. Chem. B 109 (2005) 18535.
[46] M. Aschoff, S. Speller, J. Kuntze, W. Heiland, E. Platzgummer, M. Schmid, P. Varga, B. Baretzky, Surf. Sci. 415 (1998) L1051.
[47] M. Aschoff, G. Piaszenski, S. Speller, W. Heiland, Surf. Sci. 402–404 (1998) 770.
[48] H. Niehus, W. Heiland, E. Taglauer, Surf. Sci. Rep. 17 (1993) 213.
[49] H. Niehus, Phys. Status Solidi B 192 (1995) 357.
[50] S. Schomann, E. Taglauer, Surf. Rev. Lett. 3 (1996) 1823.
[51] L. Houssiau, P. Bertrand, Nucl. Instrum. Methods B 125 (1997) 328.
[52] B.E. Koel, A. Sellidj, M.T. Paffett, Phys. Rev. B. 46 (1992) 7846.
[53] A.W. Stephenson, C.J. Baddeley, M.S. Tikhov, R.M. Lambert, Surf. Sci. 398 (1998) 172.
[54] F. Maroun, F. Ozanam, O.M. Magnussen, R.J. Bhem, Science 293 (2001) 1811.
[55] T.G. Owens, T.E. Jones, T.C.Q. Noakes, P. Bailey, C.J. Baddeley, J. Phys. Chem. B 110 (42) (2006) 21152.
[56] M. Bowker, C. Morgan, J. Couves, Surf. Sci. 555 (2004) 145.
[57] M. Bowker, C. Morgan, Catal. Lett. 98 (2004) 67.
[58] M. Bowker, C. Morgan, N. Perkins, R. Holroyd, E. Fourre, F. Grillo, A. MacDowall, J. Phys. Chem. B 109 (2005) 2377.
[59] Y.F. Han, D. Kumar, C. Sivadinarayana, D.W. Goodman, J. Catal. 224 (2004) 60.
[60] K. Luo, T. Wei, C.W. Yi, S. Axnanda, D.W. Goodman, J. Phys. Chem. B 109 (2005) 23517.
[61] M.S. Chen, K. Luo, Z. Wei, Z. Yan, D. Kumar, C.-W. Yi, D.W. Goodman, Catal. Today 117 (2006) 37.
[62] N. Tsud, T. Skala, F. Sutata, K. Veltruska, V. Dudr, S. Fabik, L. Sedlacek, V. Chab, K.C. Prince, V. Matolin, Surf. Sci. 595 (2005) 138.
[63] A.F. Lee, C.J. Baddeley, M.S. Tikhov, R.M. Lambert, Surf. Sci. 373 (1997) 195.
[64] D. Kumar, M.S. Chen, D.W. Goodman, unpublished data.
[65] T. Wei, K. Luo, S. Axnanda, D.W. Goodman, in press.
[66] J.M. Peck, D.I. Mahon, B.E. Koel, Surf. Sci. 410 (1998) 200.
[67] M. Batzill, D.E. Beck, B.E. Koel, Surf. Sci. 466 (2000) L821.
[68] A.F. Lee, C.J. Baddeley, C. Hardacre, G.D. Moggridge, R.M. Ormerod, R.M. Lambert, J.P. Candy, J.-M. Basset, J. Phys. Chem. B 101 (1997) 2979.